

Research Paper

What happens to the osteoporotic bone mesenchymal stem cells? Evidence from RNA sequencing

Mingyang Li^{1*}, Rong Cong^{2*}, Huadong Wang¹, Chao Ma¹, Yongwei Lv¹, Yang Zheng¹, Yantao Zhao¹, Qin Fu^{3#}, Li Li^{1,4#}

1. Senior Department of Orthopedics, the Fourth Medical Center of PLA General Hospital, Beijing, China.
2. Senior Department of Obstetrics & Gynecology, the Seventh Medical Center of PLA General Hospital, Beijing, China.
3. Department of Orthopedics, Shengjing Hospital of China Medical University, Shenyang, China.
4. Beijing Engineering Research Center of Orthopedics Implants, Beijing, China.

* Joint first author Mingyang Li and Rong Cong contributed equally to the work.

Joint corresponding author Qin Fu and Li Li contributed equally to the work.

✉ Corresponding author: Li Li; E-mail: lili304@126.com. Qin Fu; E-mail: fuq@sj-hospital.org.

© The author(s). This is an open access article distributed under the terms of the Creative Commons Attribution License (<https://creativecommons.org/licenses/by/4.0/>). See <http://ivyspring.com/terms> for full terms and conditions.

Received: 2023.07.16; Accepted: 2023.10.04; Published: 2024.01.01

Abstract

Evidence presented that osteoporosis is closely related to the dysfunction of bone mesenchymal stem cells (BMSCs). But most studies are insufficient to reveal what actually happens to the osteoporotic BMSCs. In this study, BMSCs were harvested from ovariectomized and sham-operated rats. After checking the characteristics of rat models and stem cells, the BMSCs were carried out for RNA sequencing. Part of the findings were verified that seven mRNAs (*Abi3bp*, *Aifm3*, *Ccl11*, *Cdkn1c*, *Chst10*, *Id2*, *Vcam1*) were significantly up-regulated in osteoporotic BMSCs while seven mRNAs (*Cep63*, *Fgfr3*, *Myc*, *Omd*, *Pou2f1*, *Smarcal1*, *Timm10b*) were down-regulated. In addition, potential miRNA-mRNA and lncRNA-mRNA regulatory networks were illustrated. The changes in osteoporotic BMSCs covered a large set of biological processes, including cell viability, differentiation, immunoreaction, bone repairment and estrogen defect. This study enriched the pathophysiological mechanisms of BMSCs and osteoporosis, as well as provided dozens of attractive RNA targets for further treatment.

Keywords: bone mesenchymal stem cell; osteoporosis; RNA sequencing; mRNA; miRNA; lncRNA

Introduction

Osteoporosis (OP) is a common skeletal metabolic disease hallmarked by the loss of bone mass and the deterioration of bone microarchitecture, as the result of systemic imbalance between bone creation and resorption[1]. With the increasing of worldwide aging population, osteoporosis poses great medical and financial burden to the whole society. It's estimated that patients suffering from osteoporosis might increase to 300 million globally by 2023[2]. In particular, postmenopausal women are taking at a higher risk due to the deficit of estrogen which has great influence on the bone turnover. Antiresorptive drugs, anabolic drugs, and combination or sequential therapies are the most common treatments for osteoporosis, but it is worth noting that some frustrating adverse effects are limiting the drug safety

for long-term use, so considerable efforts should be made to improve the existing therapies[3].

Evidence has been presented that senile osteoporosis (SOP) and postmenopausal osteoporosis (PMOP) are partly caused by the dysfunction of bone mesenchymal stem cells (BMSCs), which decline in numbers as well as preferentially differentiate into adipocytes rather than osteoblasts[4]. BMSCs are thought to be vital sources of osteoblasts and maintainers of bone homeostasis. In view of their outstanding characteristics, including self-renewal ability, multipotency, low immunogenicity, homing ability and secretory ability, BMSCs are increasingly accepted as attractive seed cells in tissue regeneration to treat with osteoporosis, as well as other diseases[5-7]. Considering the enormous therapeutic

potential of BMSCs, great efforts have been given to probe what happens to the osteoporotic BMSCs. However, the study is hampered due to the long time taken to establish osteoporosis models and the inevitable senescence of BMSCs during culture[8]. Although some scholars tried to study BMSCs with osteogenic reagents or some other treatments[9], it might be insufficient to reflect the actualities happening in osteoporotic BMSCs.

The ovariectomized (OVX) rat model has been approved by the US Food and Drug Administration (FDA) to be an ideal model to illuminate PMOP[10]. In this study, we harvested BMSCs from OVX rats and sham-operated (SHAM) rats for further high-throughput RNA sequencing (RNA-seq). It's aimed to illuminate what actually happened to the osteoporotic BMSCs and help more scholars to elaborate the underlying mechanisms of BMSCs dysfunction and osteoporosis progression.

Materials and methods

Establishment of OVX and SHAM rat models

All the animal experiments were approved by the Institutional Review Committee of the Ethics Committee of Shengjing Hospital of China Medical University. A total of 24 specific pathogen-free Sprague Dawley rats (female, 8-week-old) were randomly divided into the OVX group (n=12) and the SHAM group (n=12). All the animals were housed under standard temperature and humidity, with a 12h-light/12h-dark cycle and free rodent diet. After one week of acclimatization, the OVX group rats underwent bilateral OVX through lumbodorsal vertical incision, while the SHAM group rats were resected similar sizes of adipose tissue around bilateral ovaries. 12 weeks later, the OVX and SHAM rat models were established.

Confirmation of osteoporosis model

The OVX and SHAM rats were anesthetized and executed by excessive pentobarbital sodium following the operation after 12 weeks. Blood was taken from the abdominal aorta and centrifuged at 3,000 rpm for 15 min to collect serum. Serum ALP levels were qualified following the procedure of alkaline phosphatase kit (Solarbio, Beijing, China). Bilateral femurs were fixed in 4% paraformaldehyde solution for 48h and then decalcified in 10% EDTA solution for 1 month. Afterwards, the bones were dehydrated, permeabilized and embedded in paraffin and sliced in 5 μ m thickness. The slices were stained using Hematoxylin-Eosin Staining Kit (Solarbio, China) following the instructions. The staining was observed and recorded by the microscope (Eclipse, Nikon, Japan). The metaphysis of proximal tibias were

measured by micro-CT (Y. Cheetah, YXLON, Germany) and analyzed by VG Studiomax 3.0 (Volume Graphics, Germany).

Isolation and culture of BMSCs

Bilateral femurs and tibiae collected from OVX rats and SHAM rats were dissected free of soft tissue under aseptic conditions. Then both ends of the bones were removed with scissors, and a syringe needle was inserted into the medullary cavity. All the bone marrows were flushed out using Dulbecco's Modified Eagle Medium/Nutrient Mixture F-12 (DMEM/F12, Hyclone, UT, USA) supplemented with 10% fetal bovine serum (FBS; BioInd, Kibbutz Beit Haemek, Israel) and 1% penicillin-streptomycin solution (BioInd) into cell culture dishes. The marrow mixture provided suitable environment for BMSCs culture. The cells were incubated in 5% CO₂ humidified atmosphere at 37°C. The culture medium was replaced every 2 days. When cells density reached 80%, adherent cells were digested by 0.25% trypsin (KeyGen, Nanjing, China) and passaged into new dishes.

Identification of BMSCs

According to the guidelines announced by The International Society for Cellular Therapy, BMSCs should be identified in terms of morphology, immunophenotyping and multipotency (Clinical Application of Bone Marrow Mesenchymal Stem/Stromal Cells to Repair Skeletal Tissue).

Morphology: The primary-generation and the third-generation BMSCs were washed by phosphate-buffered saline (PBS) and observed by the microscope (Eclipse, Nikon, Japan). **Immunophenotyping:** The third-generation BMSCs were harvested with trypsin, centrifuged at 1,000 r/min for 5 min, and then washed and recentrifuged by PBS twice. The cells were counted and resuspended with PBS into four tubes (1x10⁶ cells/500ul). Fluorochrome conjugated mouse anti-rat antibodies (CD29-FITC, CD45-FITC, CD90-PE, BD Pharmingen, USA) and another equivalent PBS were mixed into individual tubes. The cells were incubated in the dark at 4°C for 30min and detected by flow cytometer (BD Biosciences, USA).

Multipotency: For osteogenic differentiation, the third-generation BMSCs were seeded into cell culture plates and cultured in high glucose DMEM (HG-DMEM) medium containing 10% FBS, 10nmol/l dexamethasone, 50mg/ml ascorbic acid, and 10mmol/l b-glycerophosphate. After 14 days, cells were fixed by 4% paraformaldehyde and stained with BCIP/NBT Alkaline Phosphatase Color Development Kit (Beyotime, Beijing, China) or Alizarin Red S solution (1%, pH=4.2, Solarbio), following the

manufacturer's instructions. For adipogenic differentiation, the third-generation BMSCs were cultured in high glucose DMEM (HG-DMEM) medium containing 10% FBS, 10nmol/l dexamethasone, 0.5mmol/l 3-isobutyl-1-methylxanthine, 0.2mmol/l indomethacin, and 10ug/ml insulin. After 14 days, cells were fixed by 4% paraformaldehyde and stained with Oil Red O stain kit (Solarbio, Beijing, China) The staining was observed and recorded by the microscope (Eclipse, Nikon, Japan).

High-throughput sequencing analysis

The third-generation BMSCs collected from OVX and SHAM rats were harvested and underwent high-throughput sequencing analysis by Novogene Bioinformatics Technology Co., Ltd. (Beijing, China). The detailed procedures of RNA-seq have been described in our previous study. Cytoscape 3.9.0 (Free Software Foundation, MA, USA) was applied to describe the miRNA-mRNA networks predicted by RNA-seq.

RNA extraction and quantitation

Total RNA from OVX and SHAM BMSCs was fetched by TRIzol (Invitrogen, USA) following the manual's instructions, and then reversely transcribed into cDNA using TB Green® Premix Ex Taq™ II (Tli RNaseH Plus) (Vazyme, Nanjing, China). The cDNA was used for qRT-PCR using HiScript II Q RT SuperMix for qPCR (+gDNA wiper) (Vazyme) with ABI Prism 7500 Fast Real-Time PCR system (Applied Biosystems, StepOnePlus, USA). Glyceraldehyde phosphate dehydrogenase (GAPDH) served as normalized reference for RNA detection. The relative expression levels of RNAs were calculated by means of the comparative $2^{-\Delta\Delta C_t}$ method. All the primers were synthesized by Sangon Biotech (Shanghai, China) and the sequences were listed in Additional file Table S1. The BMSCs for verification tests were different from the RNA-seq samples.

Statistical analysis

Statistical analysis was performed SPSS 22.0 statistical software (IBM, USA) and GraphPad Prism 8 software (GraphPad, USA). Comparisons between two groups used two-tail t-test, while comparisons among multiple groups used one-way analysis of variance (ANOVA). $P < 0.05$ was considered to be of statistical significance after multiple test correction.

Results

Increased weights, decreased ALP levels and osteoporotic bones were found in OVX rats

We established the OVX and SHAM rat models

as reported in the former studies[11]. The median weight of OVX and SHAM rats before operation were 230g and 227g (n=12), respectively. There was no statistical difference in weight between the two groups (Fig. 1A). By contrast, the median weight of OVX and SHAM rats after operation were 423g and 355g, respectively. Significant increases in the weights of OVX rats were found at 3 months after the operation (Fig. 1B). After detecting the blood samples, the ALP levels in OVX rats were significantly lower than those in SHAM rats, indicating a decreased osteogenic activity in OVX rats (Fig. 1C, n=3). In Fig. 1D, thinner bone trabecula, sparser cancellous bones, wider trabecula spacing and more fatty vacuoles were found in HE staining slices from the OVX rat femurs. In Fig. 1E, micro-CT displayed sparser cancellous bones in the OVX rat tibia. The findings in OVX rats conformed to the osteoporotic appearance.

Harvested cells tallied with the identification criteria of BMSCs

Under the microscope, both OVX BMSCs and SHAM BMSCs adhered to the surface of culture dishes and presented typical spindle shapes with gathering in volute shapes. Notably, more fatty vacuoles were flushed out into the OVX culture dishes (Fig. 2A) and the third-generation OVX BMSCs became less regular in shapes (Fig. 2B). Moreover, it was observed that OVX BMSCs were growing more sparsely than the SHAM BMSCs, and the proliferation rate of OVX BMSCs was obviously slower than the SHAM BMSCs.

Flow cytometry analysis (Fig. 2C, n=3) showed that the SHAM BMSCs carrying CD29 and CD90 accounted for 99.80% and 99.52% of the total cells, respectively, while cells carrying CD45 accounted for 0.92%. By contrast, the OVX BMSCs carrying CD29 and CD90 accounted for 97.31% and 95.26% of the total cells, respectively, while cells carrying CD45 accounted for 4.02%. The results indicated that both OVX BMSCs and SHAM BMSCs were positive for CD29 and CD90 surface markers, and negative for CD45.

Fig. 2D-F presented that Alkaline Phosphatase, Alizarin Red S and Oil Red O staining in both OVX BMSCs and SHAM BMSCs were positive, indicating that the cells could differentiate into osteoblasts and adipocytes. Moreover, the areas of NBT-formazan and mineralization nodes in OVX BMSCs were smaller than those in SHAM BMSCs, while the amounts of red fatty vacuoles in OVX BMSCs were more than those in SHAM BMSCs, indicating that OVX BMSCs were inclined to adipogenic differentiation instead of osteogenic differentiation.

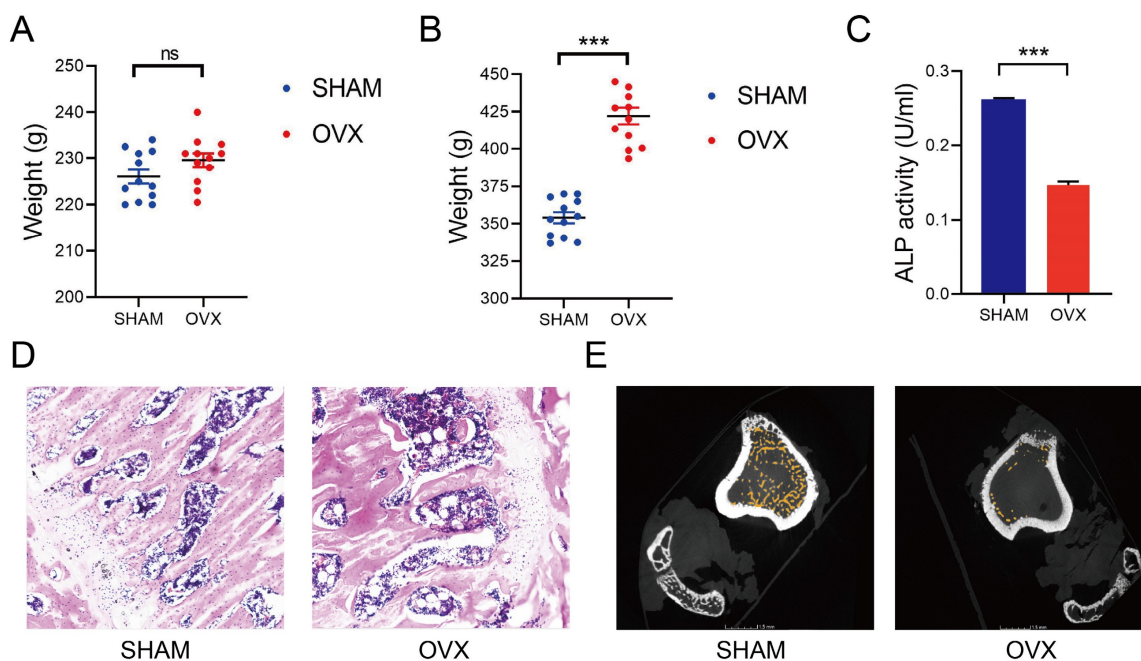


Figure 1. Establishment of OVX and SHAM rat models. **A)** The weight of OVX and SHAM rats before operation. **B)** The weight of OVX and SHAM rats at 12 weeks after operation. **C)** The ALP activity of OVX and SHAM rats at 12 weeks after operation. **D)** The HE staining of OVX and SHAM rats femurs at 12 weeks after operation. **E)** The micro-CT photos of OVX and SHAM rats tibias at 12 weeks after operation.

The comparison on morphology, immunophenotyping and multipotency proved that the harvested cells tallied with the identification criteria of BMSCs.

RNA-seq and qRT-PCR verified fourteen differentially expressed mRNAs

The RNA-seq results were displayed as a heatmap in Fig. 3A showing the significantly differentially expressed mRNAs. In total, 1998 mRNAs were found relatively down-regulated in OVX BMSCs comparing with SHAM BMSCs while 2204 mRNAs were up-regulated in some ways ($n=3$, $P<0.05$, $|\text{fold change}|>1.5$). Based on the findings, 24 pairs of PCR primers were synthesized and underwent quality testing. Excluding 10 debased or insignificant pairs, fourteen eligible mRNA primers were chosen for further study. The primer sequences are listed in Table S1. We performed qRT-PCR for verification and confirmed that seven of the mRNAs (Timm10b, Pou2f1, Myc, Cep63, Smarcal1, Fgfr3, Omd) were relatively down-regulated in OVX BMSCs while the other seven mRNAs (Abi3bp, Id2, Ccl11, Chst10, Vcam1, Aifm3, Cdkn1c) were relatively up-regulated (Fig. 3B, $n=3$). The heatmap drawing the relative expression of the fourteen mRNAs in RNA-seq was displayed in Fig. 3C, the trend of which generally matched with Fig. 3B.

RNA-seq predicted potential miRNA-mRNA and lncRNA-mRNA regulatory networks

The RNA-seq also found some differentially expressed miRNAs and lncRNAs whose expression

levels were significantly connected to the mRNAs' levels. A potential miRNA-mRNA regulatory network was displayed in Fig. 4A. Fgfr3 had the most miRNA targets. Aifm3 and Fgfr3 shared the same miRNA target, miR-6328. Chst10 and Id2 shared the same miRNA target, miR-455-3p. Abi3bp, Cep63 and Smarcal1 didn't match proper targeted miRNAs. A potential lncRNA-mRNA regulatory network was displayed in Fig. 4B. Cep63 had the most lncRNA targets. Vcam1 and Chst10 shared nine lncRNAs. Omd only matched one lncRNA. As most of the lncRNAs were not annotated, we provided the lncRNAs sequences in Table S2. The circle sizes of the lncRNAs in Fig. 4B were in line with the Pearson's correlation (absolute values between 0.97 to 1).

Discussion

As the global aging problem becomes increasingly prevalent, osteoporosis, particularly PMOP affects millions of people worldwide and imposes great socioeconomic burden[12]. The present first-line agents, including bisphosphonates (BPS), selective estrogen receptor modulators (SERM), parathyroid hormone (PTH) and denosumab, might inevitably lead to a series of adverse effects, such as myasthenia gravis, osteonecrosis and tumorigenesis, along with long-term usage in treatment of osteoporosis[3]. It is of utmost importance to find a safe and efficient alternative therapy, while BMSCs become a hotspot.

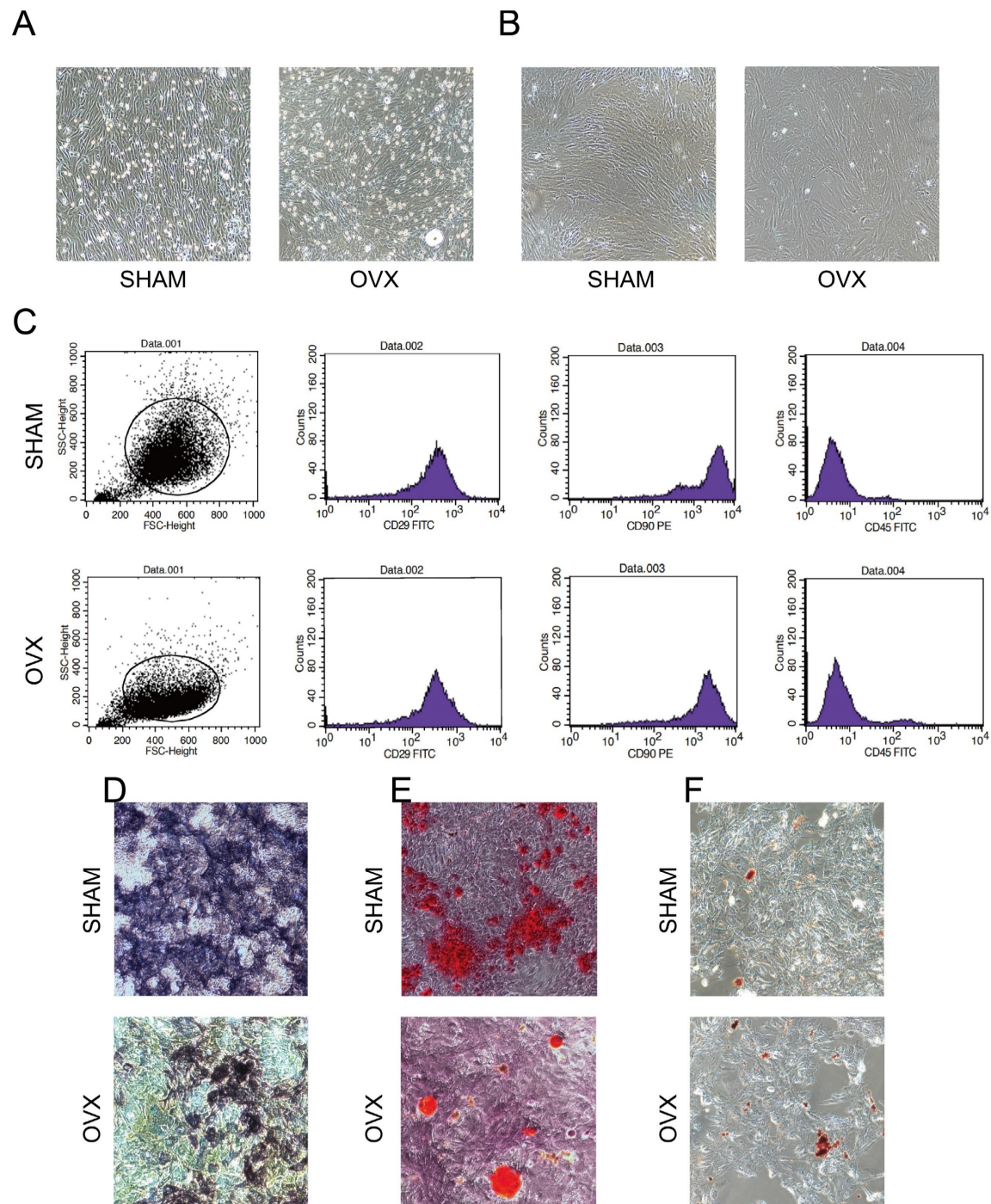


Figure 2. Identification of BMSCs. **A)** The morphology of primary OVX and SHAM BMSCs. **B)** The morphology of third-generation OVX and SHAM BMSCs. **C)** The immunophenotyping of OVX and SHAM BMSCs. **D)** The Alkaline Phosphatase staining of OVX and SHAM BMSCs after culturing in osteogenic medium for 14 days. **E)** The Alizarin Red S staining of OVX and SHAM BMSCs after culturing in osteogenic medium for 14 days. **F)** The Oil Red O staining of OVX and SHAM BMSCs after culturing in adipogenic medium for 14 days.

Accumulating evidence indicates that BMSCs present lower osteogenic capability but higher adipogenic capability in cases of aging or ovariectomy, leading to the dysfunction of bone formation and finally osteoporosis[13]. Their findings are in line with our staining assays in Fig. 2D-F that the areas of mineralization nodes in OVX BMSCs were smaller than those in SHAM BMSCs, while the amounts of red

fatty vacuoles in OVX BMSCs were more than those in SHAM BMSCs. Thus a lot of studies are trying regulating the proliferation or differentiation of BMSCs to promote osteogenesis. However, few studies chose to compare the differences between the osteoporosis individuals and the normal ones to probe into the underlying pathogenic mechanisms. Although some scholars investigated the expression

profiles of RNAs in peripheral blood of PMOP patients respectively[14-15]. The changes in blood might fail to figure out what exactly happened to BMSCs. Geng found some differentially expressed RNAs from BMSCs of SOP patients, but further studies might be limited by the acquirement of human BMSCs and ethics approval[16]. It's worth noting that the OVX rat has been taken as an ideal model to illuminate PMOP as approved by FDA[10]. Yousefzadeh provided a practical guide for inducing OVX models and introduced that the model was suitable for mimicking the estrogen deficiency-induced bone loss and showing clinical manifestations of postmenopausal osteoporosis[17]. Thus our study harvested the BMSCs from OVX and SHAM rats and performed RNA-seq. Considering the highly conservation characteristics of mRNA, this study could help find out some crucial changes during the

development of osteoporosis and provide some significant targets for treatment of osteoporosis.

Thus, firstly we established osteoporosis rat models as approved by FDA. The weights of OVX rats were significantly higher than the SHAM rats, which might attribute to the lack of estrogen. Estrogen depletion led to disturbances in lipid metabolism and caused fat accumulation and overweight[18]. The HE staining of femurs and the observation of first-generation BMSCs also revealed increasing fatty vacuoles in OVX rats. Meanwhile, the lack of estrogen led to the attenuated regenerative competence of BMSC and impairment of bone formation[19], which supported our findings that the declined ALP levels in blood and sparse cancellous bones in HE staining and micro-CT in OVX rats. Thus we successfully established the OVX and SHAM models.

According to the guidelines of The International

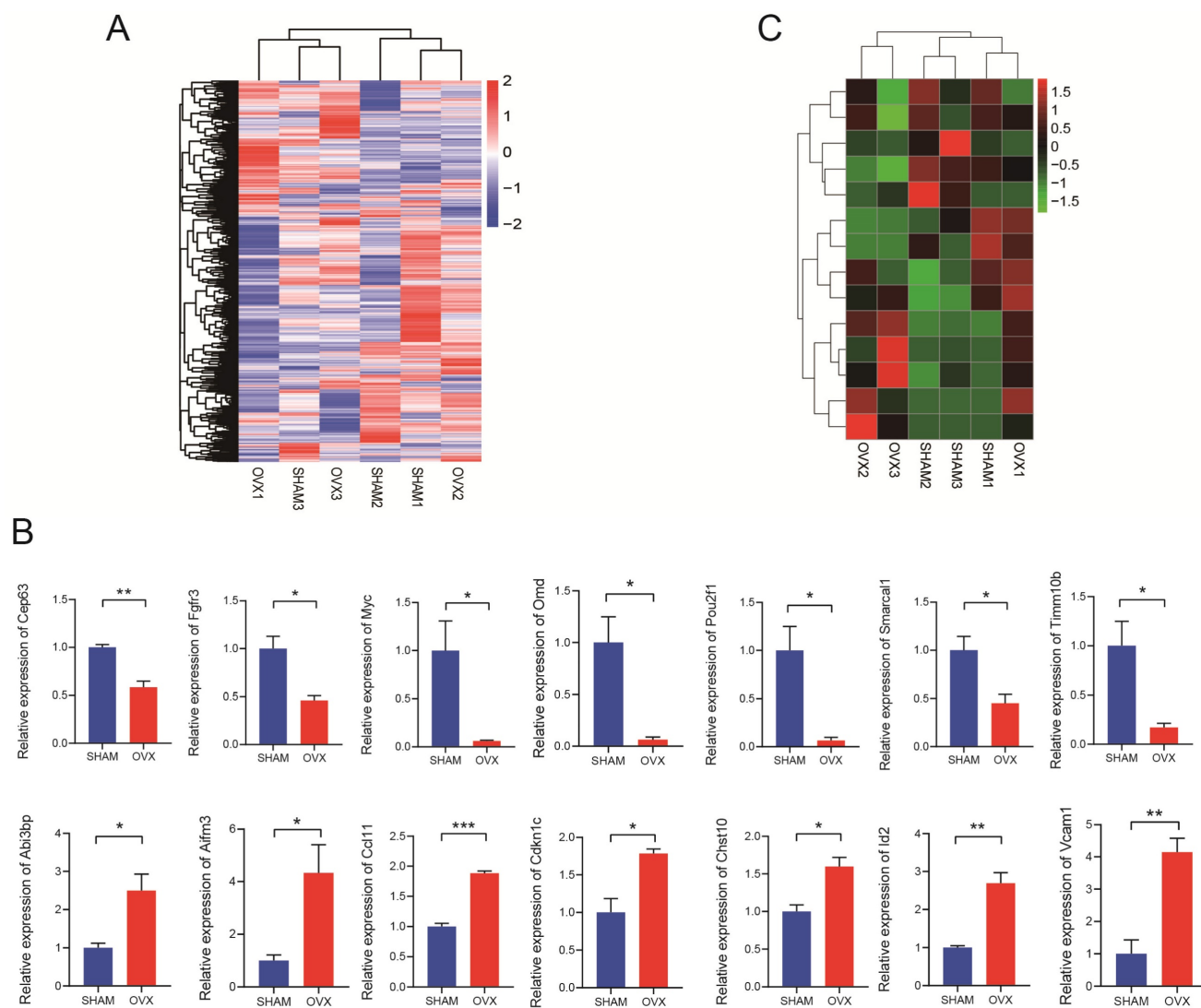


Figure 3. Analysis of RNA sequencing. **A**) The hierarchical clustering heatmap of differentially expressed mRNAs in OVX and SHAM BMSCs. **B**) Relative expression of the mRNAs (Cep63, Fgfr3, Myc, Omd, Pou2f1, Smarcal1, Timm10b, Abi3bp, Aifm3, Ccl11, Cdkn1c, Chst10, Id2 and Vcam1) in OVX and SHAM BMSCs. **C**) The relative expression of the mRNAs (Cep63, Fgfr3, Myc, Omd, Pou2f1, Smarcal1, Timm10b, Abi3bp, Aifm3, Ccl11, Cdkn1c, Chst10, Id2 and Vcam1) in the RNA-seq.

Society for Cellular Therapy, the MSCs should be characterized by: stem-like morphology, specific positive and negative immunophenotype, and multi-differentiation potency. Under the microscope, the BMSCs presented typical spindle shapes with gathering in volute shapes. Flow cytometry analysis showed that the cells were positive for CD29 and CD90, and negative for CD45. The results are consistent with existing evidences on BMSCs surface markers[20-21]: CD29 is an adhesion marker and CD90 is a marker of undifferentiated stem cells, while the lack of CD45 means the cells are not haematopoietic cells. In addition, after treating with differentiation inducers, the cells presented osteogenic and

adipogenic differentiation ability. Taken together, the BMSCs conformed to the criteria and were reliable for performing RNA-seq.

Based on the analysis of RNA-seq, we chose some of the differentially expressed mRNAs for verification via qRT-PCR. It's confirmed that seven of the mRNAs (Timm10b, Pou2f1, Myc, Cep63, Smarcal1, Fgfr3, Omd) were relatively down-regulated in OVX BMSCs while the other seven mRNAs (Abi3bp, Id2, Ccl11, Chst10, Vcam1, Aifm3, Cdkn1c) were relatively up-regulated. The trends in Fig. 3B were in line with the heatmap generated by RNA-seq in Fig. 3C.

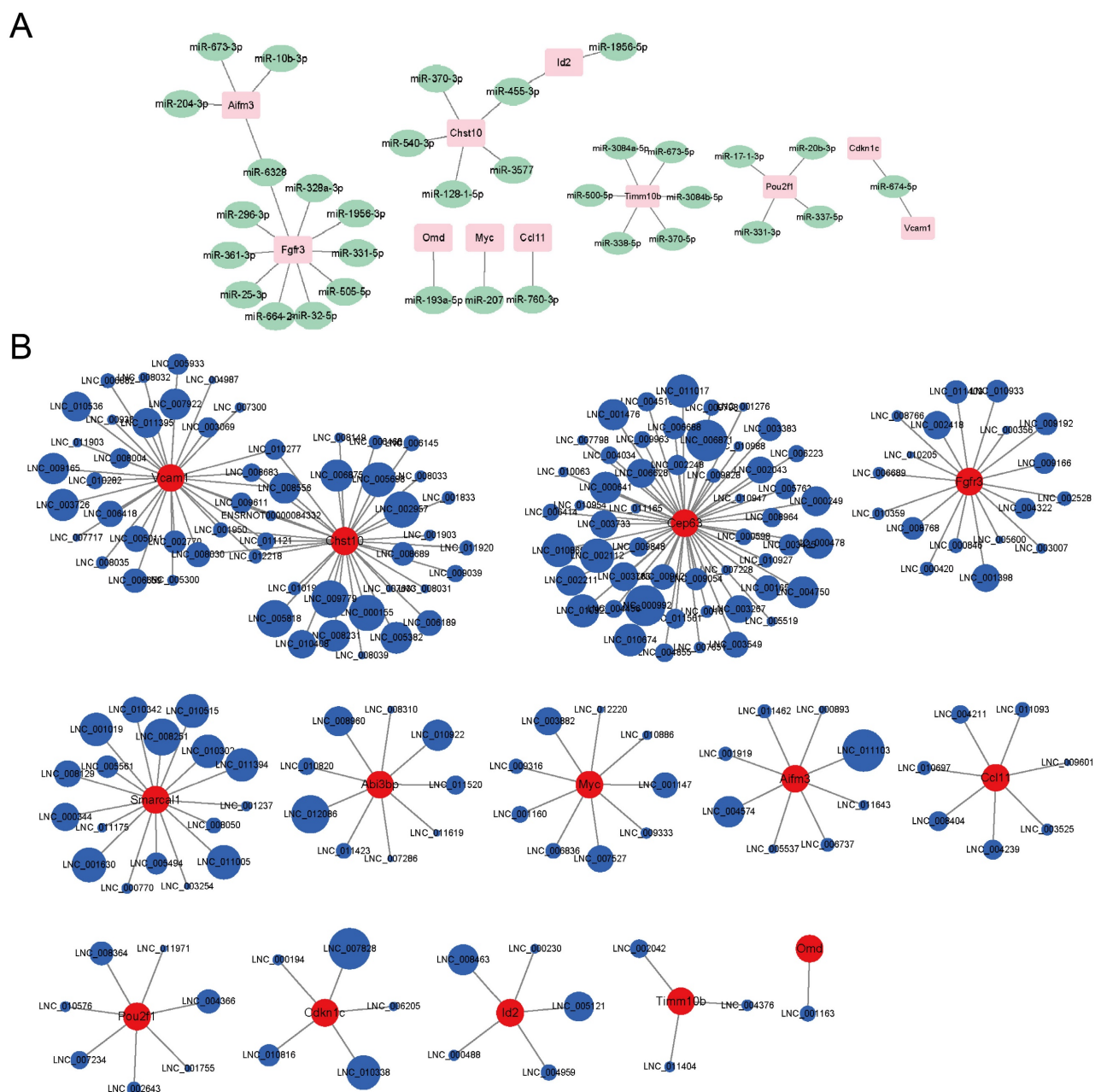


Figure 4. Potential miRNA-mRNA and lncRNA-mRNA networks. **A)** The potential miRNA-mRNA regulatory network analyzed by the RNA-seq. **B)** The potential lncRNA-mRNA regulatory network analyzed by the RNA-seq.

Some of the targets have been well studied, such as *Myc*, *Fgfr3*, *Abi3bp* and *Omd*. *Myc* (*MYC* proto-oncogene, bHLH transcription factor) is a well-known oncogene. Via FGF/FGFR signaling, it promotes MSCs proliferation, and attenuates rather than abrogates their differentiation[22]. The protein *MYC* forms a heterodimer with *MAX* to activate transcription while *MAX* also forms another heterodimer with *MAD* to antagonize *MYC/MAX* activation aiming at the same targets. The heterodimers regulates the fate of cells between proliferation (*MYC/MAX*) and differentiation (*MAX/MAD*)[23]. Decline of *Myc* in osteoporotic BMSCs might interfere their proliferation. *Fgfr3* (fibroblast growth factor receptor 3) belongs to the highly conserved FGFR family. Its protein binds to fibroblast growth hormone and participates in skeletal development through a cascade of downstream signals, especially through the ERK and p38 pathways[24]. Activated *Fgfr3* enhances the proliferation of osteoblast progenitors and promotes bone formation in mouse models, while anti-*Fgfr3* treatment blocks BMSC proliferation and osteogenic differentiation[25]. *Abi3bp* (*ABI* family member 3 binding protein) encodes an extracellular/interstitial matrix protein, which takes part in membrane ruffling and lamellipodia formation and thus influences cell-substrate adhesion and cell motility[26]. It is considered as a tumor suppressor that suppressed cell proliferation, migration and invasion[27]. Hodgkinson found *Abi3bp*-knockout increased BMSC proliferation but limited their motility and ability of osteogenic and adipogenic differentiation, indicating that *Abi3bp* played a role in switching BMSCs between proliferative and differentiating states[28]. *Omd* (osteomodulin, also known as osteoadherin; *OSAD*; *SLRR2C*) encodes a keratan sulfate proteoglycan and usually highly expressed in mineralized tissues[29]. The protein binds to *BMP2* via its terminal leucine-rich repeats and thus promotes *BMP/SMAD* signal activation, osteogenesis-associated gene transcription and mineralized nodule formation[30]. It's reported that *Omd* levels rose by 35 folds in dental pulp stem cells at the late stage of osteogenic differentiation[31]. Thus lacking *Omd* in osteoporotic BMSCs weakened their osteogenic differentiation.

Some of the other targets might have influence on osteogenic differentiation, including *Timm10b* and *Pou2f1*. *Timm10b* (translocase of inner mitochondrial membrane 10B, also known as *Fxc1*, *Tim9b*, *Tim10B*) is a member of the evolutionarily conserved *Tim* family, whose protein locates in the mitochondrial intermembrane space. The hetero-oligomeric *TIM9-10* complex hand over the carrier precursors carrying hydrophobic proteins to its membrane-associated

TIM9-10-12 complex, which is tightly associated with the *TIM22* complex in the inner membrane. Then the proteins are inserted into the mitochondrial inner membrane along *TIM22* in a dynamic manner following the membrane potential[32]. One study found that it increased 3-4 folds during the production and deposition of matrix proteins along the osteogenic differentiation of MC3T3 cells, but the mechanisms were not studied[33]. *Pou2f1* (*POU* class 2 homeobox 1, also known as *OCT1*) is a member of the *POU* transcription factor family that regulates transcription via binding to the octameric sequence *ATGCAAAT* found in the promoters and enhancers of diverse genes. It stimulates *RUNX2* recruitment to the β -casein promoter by interacting with the C-terminal region of *RUNX2* and thus relieves the autoinhibition of *RUNX2* and regulate bone development[34]. It can be modulated by *AMPK* signaling and acts on the promoter region of *miR-451a* to regulate osteoblast differentiation and mineralization[35]. Taken together, inadequate *Timm10b* and *Pou2f1* in osteoporotic BMSCs harmed osteogenic differentiation.

Some of the targets might have influence on cell viability, including *Cep63*, *Smarcal1* and *Aifm3*. *Cep63* (entrosomal protein 63) encodes a protein making up part of the annular structural base of the centrosome. It promotes the replication of centrioles and mitosis, linking the centrosome and the cell-cycle machinery via recruitment for *CDK1*[36]. Knockdown of *Cep63* leads to centrosomal distortion, chromosomal entanglement and telomere clustering defects, resulting in cell cycle arrest in the S phase[37]. The role of *Cep63* in osteology hasn't achieved much attention. Mutations in *Cep63* cause Seckel syndrome, a skeletal disease characterized by microcephaly and dwarfism, indicating a potential connection between *Cep63* and bone formation[38]. *Smarcal1* (*SWI/SNF* related, matrix associated, actin dependent regulator of chromatin, subfamily a like 1) is a member of the *SWI/SNF* family, whose protein presents helicase and *ATPase* activities and regulates gene transcription by altering the chromatin structure around the gene. It takes replication protein A off DNA and anneals complementary strands, as well as keeps replication fork and genome stabilization[39]. Downregulation of *Smarcal1* leads to transcriptional repression and G2/M checkpoint overriding, leading to mitotic abnormalities[40], and the damage remains observed beyond stem cell differentiation[41]. Mutations in *Smarcal1* also cause severe skeletal disorders, such as *Schimke immuno-osseous dysplasia (SIOD)*, characterized by growth defects, immune deficiencies and other complex appearance[42]. Lack of *Cep63* and *Smarcal1* might affect osteoporotic BMSCs viability

and the mechanisms deserved more study. Aifm3 (apoptosis inducing factor mitochondria associated 3, also known as AIFL) induces cell apoptosis in a caspase-dependent manner by changing the oxidoreductase activity and mitochondrial membrane potential[43]. It's reported that MSC-derived exosomes protect cardiomyocytes from apoptotic cell death via downregulated Aifm3[44]. However, apoptosis usually presents two-sidedness in regulating the life-death balance: higher Aifm3 levels are found associated with shorter overall survival in breast cancer, while Aifm3 also decreases stem-like properties of breast cancer stem cells and has potential to suppress tumor progression[45-46]. Aifm3 might play similar roles in BMSCs apoptosis comparing with tumor stem cells[47], but the molecular functions haven't been set forth clearly.

Evidence has found that estrogen deficiency affects the level of inflammation which contributes a lot to osteoporosis. The inflammation microenvironment affects cellular physiological processes and leads to cellular senescence. Senescent BMSCs can't function normally and will secrete more inflammatory cytokines forming a vicious circle[48]. Vcam1 (vascular cell adhesion molecule 1) is a member of the Ig superfamily, which is up-regulated in response to inflammatory cytokines such as tumor necrosis factor-alpha (TNF- α)[49]. It is a principle adhesion molecule in the interaction between HSPCs (hematopoietic stem and progenitor cells) and BMSCs[50]. Burja used inflammatory cytokines to stimulate different kinds of MSCs and found BMSCs expressed the highest levels of Vcam1. In return, the increased Vcam1 in BMSCs strengthened the interaction with HSPCs and hindered HSPC mobilization, leading to a systemic immunodeficiency[51]. Moreover, Vcam1 repressed the MURF1-mediated ubiquitylation of PPAR γ 2 and maintained PPAR γ 2 stabilization, which enhanced adipogenesis and consequently reduced osteogenesis of BMSCs[52]. Ccl11 (C-C motif chemokine ligand 11) is an anti-microbial eosinophil-specific chemokine involving in immunoregulatory and inflammatory processes, which induces cell chemotaxis and angiogenesis[53]. Studies have reported that serum Ccl11 levels elevate in rheumatoid arthritis patients and osteoarthritis patients[54]. The accumulation of Ccl11 increases preosteoclasts migration and promotes osteoclastic bone resorption[55]. Comparing with healthy subjects, serum levels of Ccl11 in osteopenia and osteoporosis patients significantly increased[56], which is in line with our findings in osteoporotic BMSCs.

Some targets have multiple functions. Id2 (inhibitor of DNA binding 2) belongs to the ID family,

a group of helix-loop-helix (HLH) transcriptional regulators. Basic HLH transcriptional regulators usually have an HLH domain, which allows proteins to homodimerize or heterodimerize and recruit complexes to act with DNA, and a basic domain, which is essential for binding with DNA. But the ID family lacks of the basic domain. Thus the family can't bind to DNA directly but binds to other basic HLH transcription factors in a dominant-negative manner, preventing them from binding and interacting with DNA[57]. It is found that Id proteins promote the proliferation of osteoblast progenitor cells but they must be down-regulated during the late stage of osteogenic differentiation[58]. Similarly, Id2 has been found to promote self-renewal of MSC and suppresses osteolineage commitment[59]. Thus high levels of ID2 in osteoporotic BMSCs might fail to activate osteogenesis. In addition, Id2 strongly promotes osteoclastogenesis in rheumatoid arthritis models[60], indicating it might strengthen osteoclasts in some way. Chst10 (carbohydrate sulfotransferase 10, also known as HNK1ST) encodes a sulfotransferase targeting to the human natural killer-1 (HNK-1) glycan and contributing to the HNK-1 carbohydrate biosynthesis[61]. HNK-1 was present in the osteoblasts, osteocytes and osteogenic cells during maxillaries osteogenesis and bone defect repairment[62]. Thus Chst10 might contribute to bone repair when osteoporosis happens. Evidence also found Chst10 modulate cell adhesion, recognition and migration[63]. Misa Suzuki-Anekoji generated Chst10-deficient mutant mice and found serum estrogen levels in Chst10-deficient mice were higher than in wild-type mice, suggesting that Chst10 could regulate steroid hormone through glucuronidation[64]. The changes of Chst10 in OVX BMSCs might also attribute to the lack of estrogen. The underlying mechanisms deserve further study.

Taken together, the pathogenesis of PMOP is a complex process. Changes have been found affecting cell differentiation and viability, or in response to inflammation, bone repairment and estrogen defect. In addition, the RNA-seq also found some differentially expressed miRNAs and lncRNAs that might interact with above mRNA targets. MiRNAs usually act as a negative regulator over the process of gene expression by either mRNA degradation or translational inhibition[65]. Some of the miRNAs have been well studied. For example, Hu found miR-1224-5p was positively correlated with fracture healing progression and identified miR-1224-5p as a key bone osteogenic regulator by targeting ADCY2 via the Rap1-signaling pathway[66]. But the roles of most of the miRNAs remain unclear. LncRNAs are commonly found as competitive endogenous RNAs to

sponge miRNAs and modulates downstream mRNAs function. For example, Wu found lncRNA SERPINB9P1 regulated BMSCs osteogenic differentiation via altering SIRT6 mRNA levels through its suppression on miR-545-3p[67]. However, most of the lncRNAs are found by RNA-seq for the first time and their functions are not annotated. We provided the lncRNAs sequences in supplementary file in anticipation of extensive studies.

Limited by the difficulties in harvesting BMSCs from OVX samples, we haven't tested and verified the differentially expressed miRNAs and lncRNAs as well as possible networks. We hope our findings could be a rich source of inspiration for more scholars. In addition, for similar reasons, we didn't have enough cells to compare the protein levels of above targets between OVX and SHAM samples. In the following studies, we will cover the shortage and deeply study the underlying mechanism of each target to make the findings more reliable.

In conclusion, benefit from RNA-seq technology, we compared the differentially expressed RNAs from OVX and SHAM BMSCs. 7 up-regulated (Abi3bp, Aifm3, Ccl11, Cdkn1c, Chst10, Id2, Vcam1) and 7 down-regulated (Cep63, Fgfr3, Myc, Omd, Pou2f1, Smarcal1, Timm10b) mRNAs in osteoporotic BMSCs were proven by qRT-PCR. In addition, potential miRNA-mRNA and lncRNA-mRNA networks were illustrated. The changes were found covering a large set of biological processes, including cell viability, differentiation, immunoreaction, bone repairment and estrogen defect. This study enriched the pathophysiological mechanisms of PMOP and provided dozens of attractive RNA targets in treatment of osteoporosis for further study.

Supplementary Material

Supplementary tables.

<https://www.medsci.org/v21p0095s1.pdf>

Acknowledgements

We are grateful for the supported from the laboratories in the Fourth Medical Center of PLA General Hospital and Shengjing Hospital of China Medical University.

Funding

This research received no specific grant from any funding agency in the public, commercial or not-for-profit sectors.

Data availability

All the data that support the findings of this study are available from the corresponding author upon reasonable request.

Competing Interests

The authors have declared that no competing interest exists.

References

- Brown JP. Long-Term Treatment of Postmenopausal Osteoporosis. *Endocrinol Metab (Seoul)*. 2021 Jun;36(3):544-552.
- Chen W, Zhang B, Chang X. Emerging roles of circular RNAs in osteoporosis. *J Cell Mol Med*. 2021;25:9089-101.
- LeBoff MS, Greenspan SL, Insogna KL, Lewiecki EM, Saag KG, Singer AJ, Siris ES. The clinician's guide to prevention and treatment of osteoporosis. *Osteoporos Int*. 2022 Oct;33(10):2049-2102.
- Lai G, Zhao R, Zhuang W, Hou Z, Yang Z, He P, Wu J, Sang H. BMSC-derived exosomal miR-27a-3p and miR-196b-5p regulate bone remodeling in ovariectomized rats. *PeerJ*. 2022 Sep 22;10:e13744.
- Chen H, Zhou L. Treatment of ischemic stroke with modified mesenchymal stem cells. *Int J Med Sci*. 2022 Jun 27;19(7):1155-1162.
- Zhang Y, Zhou L, Fu Q, Liu Z. ANKRD1 activates the Wnt signaling pathway by modulating CAV3 expression and thus promotes BMSC osteogenic differentiation and bone formation in ovariectomized mice. *Biochim Biophys Acta Mol Basis Dis*. 2023 Jun;1869(5):166693.
- Malekpour K, Hazrati A, Zahar M, Markov A, Zekiy AO, Navashenaq JG, et al. The Potential Use of Mesenchymal Stem Cells and Their Derived Exosomes for Orthopedic Diseases Treatment. *Stem Cell Rev Rep*. 2022;18:933-51.
- Xiao HH, Yu X, Yang C, Chan CO, Lu L, Cao S, Wan SW, Lan ZJ, Mok DK, Chen S, Wong M. Prenylated Isoflavonoids-Rich Extract of Erythrinae Cortex Exerted Bone Protective Effects by Modulating Gut Microbial Compositions and Metabolites in Ovariectomized Rats. *Nutrients*. 2021 Aug 25;13(9):2943.
- Chen SC, Jiang T, Liu QY, Liu ZT, Su YF, Su HT. Hsa_circ_0001485 promoted osteogenic differentiation by targeting BMPR2 to activate the TGFβ-BMP pathway. *Stem Cell Res Ther*. 2022 Sep 5;13(1):453. doi: 10.1186/s13287-022-03150-1.
- Thompson DD, Simmons HA, Pirie CM, Ke HZ. FDA Guidelines and animal models for osteoporosis. *Bone*. 1995 Oct;17(4 Suppl):125S-133S.
- Li M, Cong R, Yang L, Yang L, Zhang Y, Fu Q. A novel lncRNA LNC_000052 leads to the dysfunction of osteoporotic BMSCs via the miR-96-5p-PIK3R1 axis. *Cell Death Dis*. 2020 Sep 23;11(9):795.
- Arceo-Mendoza RM, Camacho PM. Postmenopausal Osteoporosis: Latest Guidelines. *Endocrinol Metab Clin North Am*. 2021 Jun;50(2):167-178.
- Li H, Qu J, Zhu H, Wang J, He H, Xie X, et al. CGRP Regulates the Age-Related Switch Between Osteoblast and Adipocyte Differentiation. *Front Cell Dev Biol*. 2021;9:675503.
- Chen T, Huo K, Kong D, Su S, Yang T, Zhang W, Shao J. Comprehensive analysis of lncRNA expression profiles in postmenopausal osteoporosis. *Genomics*. 2022 Sep;114(5):110452.
- Chen X, Yang L, Ge D, Wang W, Yin Z, Yan J, Cao X, Jiang C, Zheng S, Liang B. Long non-coding RNA XIST promotes osteoporosis through inhibiting bone marrow mesenchymal stem cell differentiation. *Exp Ther Med*. 2019 Jan;17(1):803-811. doi: 10.3892/etm.2018.7033.
- Geng Y, Chen J, Chang C, Zhang Y, Duan L, Zhu W, Mou L, Xiong J, Wang D. Systematic Analysis of mRNAs and ncRNAs in BMSCs of Senile Osteoporosis Patients. *Front Genet*. 2021 Dec 20;12:776984. doi: 10.3389/fgene.2021.776984.
- Yousefzadeh N, Kashfi K, Jeddi S, Ghasemi A. Ovariectomized rat model of osteoporosis: a practical guide. *EXCLI J*. 2020 Jan 10;19:89-107.
- Guo M, Cao X, Ji D, Xiong H, Zhang T, Wu Y, Suo L, Pan M, Brugger D, Chen Y, Zhang K, Ma B. Gut Microbiota and Acylcarnitine Metabolites Connect the Beneficial Association between Estrogen and Lipid Metabolism Disorders in Ovariectomized Mice. *Microbiol Spectr*. 2023 May 4:e0014923.
- Zhang X, Liu L, Liu D, Li Y, He J, Shen L. 17β-Estradiol promotes angiogenesis of bone marrow mesenchymal stem cells by upregulating the PI3K-Akt signaling pathway. *Comput Struct Biotechnol J*. 2022 Jul 19;20:3864-3873.
- Liang Y, Zhou R, Liu X, You L, Chen C, Ye X, Wei W, Liu J, Dai J, Li K, Zhao X. Leukemia Inhibitory Factor Facilitates Self-Renewal and Differentiation and Attenuates Oxidative Stress of BMSCs by Activating PI3K/AKT Signaling. *Oxid Med Cell Longev*. 2022 Sep 5;2022:5772509.
- Zhang Z, Zhou F, Zheng J, Mu J, Bo P, You B. Preparation of myocardial patches from Dil-labeled rat bone marrow mesenchymal stem cells and neonatal rat cardiomyocytes contact co-cultured on polycaprolactone film. *Biomed Mater*. 2022 May 27;17(4).

22. Melnik S, Werth N, Boeuf S, Hahn EM, Gotterbarm T, Anton M, et al. Impact of c-MYC expression on proliferation, differentiation, and risk of neoplastic transformation of human mesenchymal stromal cells. *Stem Cell Res Ther.* 2019;10:73.
23. Karadkhelkar NM, Lin M, Eubanks LM, Janda KD. Demystifying the Druggability of the MYC Family of Oncogenes. *J Am Chem Soc.* 2023 Feb 15;145(6):3259-3269.
24. Narayana J, Horton WA. FGFR3 biology and skeletal disease. *Connect Tissue Res.* 2015;56:427-33.
25. Mohan S, Muthusamy K, Nagamani S, Kesavan C. Computational prediction of small molecules with predicted binding to FGFR3 and testing biological effects in bone cells. *Exp Biol Med (Maywood).* 2021;246:1660-7.
26. Delfin DA, DeAguero JL, McKown EN. The Extracellular Matrix Protein ABI3BP in Cardiovascular Health and Disease. *Front Cardiovasc Med.* 2019;6:23.
27. Cai H, Li Y, Qin D, Wang R, Tang Z, Lu T, et al. The Depletion of ABI3BP by MicroRNA-183 Promotes the Development of Esophageal Carcinoma. *Mediators Inflamm.* 2020;2020:3420946.
28. Hodgkinson CP, Naidoo V, Patti KG, Gomez JA, Schmeckpeper J, Zhang Z, et al. Abi3bp is a multifunctional autocrine/paracrine factor that regulates mesenchymal stem cell biology. *Stem Cells.* 2013;31:1669-82.
29. Hamaya E, Fujisawa T, Tamura M. Osteoadherin serves roles in the regulation of apoptosis and growth in MC3T3E1 osteoblast cells. *Int J Mol Med.* 2019;44:2336-44.
30. Lin W, Zhu X, Gao L, Mao M, Gao D, Huang Z. Osteomodulin positively regulates osteogenesis through interaction with BMP2. *Cell Death Dis.* 2021;12:147.
31. Lin W, Gao L, Jiang W, Niu C, Yuan K, Hu X, et al. The role of osteomodulin on osteo/odontogenic differentiation in human dental pulp stem cells. *Bmc Oral Health.* 2019;19:22.
32. Weinhäupl K, Wang Y, Hessel A, Brennich M, Lindorff-Larsen K, Schanda P. Architecture and assembly dynamics of the essential mitochondrial chaperone complex TIM9-10-12. *Structure.* 2021 Sep 2;29(9):1065-1073.e4.
33. Hadjiargyrou M, Halsey MF, Ahrens W, Rightmire EP, McLeod KJ, Rubin CT. Cloning of a novel cDNA expressed during the early stages of fracture healing. *Biochem Biophys Res Commun.* 1998;249:879-84.
34. Inman CK, Li N, Shore P. Oct-1 counteracts autoinhibition of Runx2 DNA binding to form a novel Runx2/Oct-1 complex on the promoter of the mammary gland-specific gene beta-casein. *Mol Cell Biol.* 2005;25:3182-93.
35. Karvande A, Kushwaha P, Ahmad N, Adhikary S, Kothari P, Tripathi AK, et al. Glucose dependent miR-451a expression contributes to parathyroid hormone mediated osteoblast differentiation. *Bone.* 2018;117:98-115.
36. Gurkaslar HK, Culfa E, Arslanhan MD, Lince-Faria M, Firat-Karalar EN. CCDC57 Cooperates with Microtubules and Microcephaly Protein CEP63 and Regulates Centriole Duplication and Mitotic Progression. *Cell Rep.* 2020;31:107630.
37. Liu C, Yu F, Ma R, Zhang L, Du G, Niu D, et al. Cep63 knockout inhibits the malignant phenotypes of papillary thyroid cancer cell line TPC1. *Oncol Rep.* 2021;46.
38. Marjanovic M, Sanchez-Huertas C, Terre B, Gomez R, Scheel JF, Pacheco S, et al. CEP63 deficiency promotes p53-dependent microcephaly and reveals a role for the centrosome in meiotic recombination. *Nat Commun.* 2015;6:7676.
39. Bansal R, Hussain S, Chanana UB, Bisht D, Goel I, Muthuswami R. SMARCAL1, the annealing helicase and the transcriptional co-regulator. *Iubmb Life.* 2020;72:2080-96.
40. Sethy R, Rakesh R, Patne K, Arya V, Sharma T, Haokip DT, et al. Regulation of ATM and ATR by SMARCAL1 and BRG1. *Biochim Biophys Acta Gene Regul Mech.* 2018;1861:1076-92.
41. Pugliese GM, Salaris F, Palermo V, Marabitti V, Morina N, Rosa A, Franchitto A, Pichierrri P. Inducible SMARCAL1 knockdown in iPSC reveals a link between replication stress and altered expression of master differentiation genes. *Dis Model Mech.* 2019 Oct 17;12(10):dmm039487.
42. Simon AJ, Lev A, Jeison M, Borochowitz ZU, Korn D, Lerenthal Y, et al. Novel SMARCAL1 bi-allelic mutations associated with a chromosomal breakage phenotype in a severe SIOD patient. *J Clin Immunol.* 2014;34:76-83.
43. Lozic M, Minarik L, Racetin A, Filipovic N, Saraga Babic M, Vukojevic K. CRKL, AIFM3, AIF, BCL2, and UBASH3A during Human Kidney Development. *Int J Mol Sci.* 2021 Aug 25;22(17):9183.
44. Cheng H, Chang S, Xu R, Chen L, Song X, Wu J, et al. Hypoxia-challenged MSC-derived exosomes deliver miR-210 to attenuate post-infarction cardiac apoptosis. *Stem Cell Res Ther.* 2020;11:224.
45. Zheng A, Zhang L, Song X, Wang Y, Wei M, Jin F. Clinical implications of a novel prognostic factor AIFM3 in breast cancer patients. *Bmc Cancer.* 2019;19:451.
46. Chua-On D, Prongvitaya T, Tummanatsakun D, Techasen A, Limpaboon T, Roytrakul S, et al. Apoptosis-Inducing Factor, Mitochondrion-Associated 3 (AIFM3) Protein Level in the Sera as a Prognostic Marker of Cholangiocarcinoma Patients. *Biomolecules.* 2020;10.
47. Urbano A, Lakshmanan U, Choo PH, Kwan JC, Ng PY, Guo K, et al. AIF suppresses chemical stress-induced apoptosis and maintains the transformed state of tumor cells. *Embo J.* 2005;24:2815-26.
48. Wu W, Fu J, Gu Y, Wei Y, Ma P, Wu J. JAK2/STAT3 regulates estrogen-related senescence of bone marrow stem cells. *J Endocrinol.* 2020;245:141-53.
49. Smith AO, Adzraku SY, Ju W, Qiao J, Xu K, Zeng L. A novel strategy for isolation of mice bone marrow endothelial cells (BMECs). *Stem Cell Res Ther.* 2021;12:267.
50. Oostendorp RA, Reisbach G, Spitzer E, Thalmeier K, Dienemann H, Mergenthaler HG, et al. VLA-4 and VCAM-1 are the principal adhesion molecules involved in the interaction between blast colony-forming cells and bone marrow stromal cells. *Br J Haematol.* 1995;91:275-84.
51. Bae J, Choi SP, Isono K, Lee JY, Park SW, Choi CY, et al. Phc2 controls hematopoietic stem and progenitor cell mobilization from bone marrow by repressing Vcam1 expression. *Nat Commun.* 2019;10:3496.
52. Liu Z, Liu H, He J, Lin P, Tong Q, Yang J. Myeloma cells shift osteoblastogenesis to adipogenesis by inhibiting the ubiquitin ligase MURF1 in mesenchymal stem cells. *Sci Signal.* 2020 May 26;13(633):eaay8203.
53. Park JY, Kang YW, Choi BY, Yang YC, Cho BP, Cho WG. CCL11 promotes angiogenic activity by activating the PI3K/Akt pathway in HUVECs. *J Recept Signal Transduct Res.* 2017 Aug;37(4):416-421.
54. Wakabayashi K, Isozaki T, Tsubokura Y, Fukuse S, Kasama T. Eotaxin-1/CCL11 is involved in cell migration in rheumatoid arthritis. *Sci Rep.* 2021;11:7937.
55. Kindstedt E, Holm CK, Sulniute R, Martinez-Carrasco I, Lundmark R, Lundberg P. CCL11, a novel mediator of inflammatory bone resorption. *Sci Rep.* 2017;7:5334.
56. Ahmadi H, Khorramdelazad H, Hassanshahi G, Abbasi FM, Ahmadi Z, Noroozi KM, et al. Involvement of Eotaxins (CCL11, CCL24, CCL26) in Pathogenesis of Osteopenia and Osteoporosis. *Iran J Public Health.* 2020;49:1769-75.
57. Cotta CV, Leventaki V, Atsaves V, Vidaki A, Schlette E, Jones D, et al. The helix-loop-helix protein Id2 is expressed differentially and induced by myc in T-cell lymphomas. *Cancer-Am Cancer Soc.* 2008;112:552-61.
58. Peng Y, Kang Q, Luo Q, Jiang W, Si W, Liu BA, et al. Inhibitor of DNA binding/differentiation helix-loop-helix proteins mediate bone morphogenetic protein-induced osteoblast differentiation of mesenchymal stem cells. *J Biol Chem.* 2004;279:32941-9.
59. Iyer S, Viernes DR, Chisholm JD, Margulies BS, Kerr WG. SHIP1 regulates MSC numbers and their osteolineage commitment by limiting induction of the PI3K/Akt/beta-catenin/Id2 axis. *Stem Cells Dev.* 2014;23:2336-51.
60. Kurowska-Stolarska M, Distler JH, Jungel A, Rudnicka W, Neumann E, Pap T, et al. Inhibitor of DNA binding/differentiation 2 induced by hypoxia promotes synovial fibroblast-dependent osteoclastogenesis. *Arthritis Rheum.* 2009;60:3663-75.
61. Kizuka Y, Matsui T, Takematsu H, Kozutsumi Y, Kawasaki T, Oka S. Physical and functional association of glucuronyltransferases and sulfotransferase involved in HNK-1 biosynthesis. *J Biol Chem.* 2006;281:13644-51.
62. Stuepp RT, Modolo F, Trentin AG, Garcez RC, Biz MT. HNK1 and Sox10 are present during repair of mandibular bone defects. *Biotech Histochem.* 2020;95:619-25.
63. Zhao X, Graves C, Ames SJ, Fisher DE, Spanjaard RA. Mechanism of regulation and suppression of melanoma invasiveness by novel retinoic acid receptor-gamma target gene carbohydrate sulfotransferase 10. *Cancer Res.* 2009;69:5218-25.
64. Suzuki-Anekoji M, Suzuki A, Wu SW, Angata K, Murai KK, Sugihara K, et al. In vivo regulation of steroid hormones by the Chst10 sulfotransferase in mouse. *J Biol Chem.* 2013;288:5007-16.
65. Ko NY, Chen LR, Chen KH. The Role of Micro RNA and Long-Non-Coding RNA in Osteoporosis. *Int J Mol Sci.* 2020 Jul 10;21(14):4886.
66. Hu L, Xie X, Xue H, Wang T, Panayi AC, Lin Z, Xiong Y, Cao F, Yan C, Chen L, Cheng P, Zha K, Sun Y, Liu G, Yu C, Hu Y, Tao R, Zhou W, Mi B, Liu G. MiR-1224-5p modulates osteogenesis by coordinating osteoblast/osteoclast differentiation via the Rap1 signaling target ADCY2. *Exp Mol Med.* 2022 Jul;54(7):961-972.

67. Wu M, Dai M, Liu X, Zeng Q, Lu Y. lncRNA SERPINB9P1 Regulates SIRT6 Mediated Osteogenic Differentiation of BMSCs via miR-545-3p. *Calcif Tissue Int.* 2023 Jan;112(1):92-102.